A BINARY CONTROL CHART TO DETECT SMALL JUMPS

Ewaryst Rafajłowicz

Institute of Computer Engineering, Control and Robotics

Wrocław University of Technology, Poland

Ansgar Steland[1]

Institute of Statistics

RWTH Aachen University, Germany

July 16th, 2008

Abstract

The classic Np chart gives a signal if the number of successes in a sequence of independent binary variables exceeds a control limit. Motivated by engineering applications in industrial image processing and, to some extent, financial statistics, we study a simple modification of this chart, which uses only the most recent observations. Our aim is to construct a control chart for detecting a shift of an unknown size, allowing for an unknown distribution of the error terms. Simulation studies indicate that the proposed chart is superior in terms of out-of-control average run length, when one is interest in the detection of very small shifts. We provide a (functional) central limit theorem under a change-point model with local alternatives which explains that unexpected and interesting behavior. Since real observations are often not independent, the question arises whether these results still hold true for the dependent case. Indeed, our asymptotic results work under the fairly general condition that the observations form a martingale difference array. This enlarges the applicability of our results considerably, firstly, to a large class time series models, and, secondly, to locally dependent image data, as we demonstrate by an example.

MSC 2000: Primary 62L10, 60F17, 62G20; Secondary 62P30, 68U10, 62P05.

1 Introduction

Detection of changes in the mean characteristic of produced items is still the most frequently used tool in quality control. A large variety of control charts have been proposed in the last fifty years. For comprehensive reviews we refer to Antoch and Jarušková (2002), Antoch, Hušková M., and Jarušková (2002), the monograph Brodsky and Darkhovsky (2000),

---

[1]Address of correspondence: Prof. Dr. A. Steland, RWTH Aachen University, Institute of Statistics, Wüllnerstr. 3, D-52056 Aachen, Germany.

and also to the articles Woodall (1997), Chakraborti, van der Laan, and Bakir (2001), and Montgomery (2001). Investigations of their properties indicate that one can not hope to select one "universally good" chart, which is uniformly sensitive to small, moderate and large shifts in the mean and still robust against violating the normality of errors assumption. On the other hand, a wide accessability of computer systems allows to run simultaneously several control charts with different sensitivity ranges for the same process. It is well known, the Shewart chart is well tuned to detect rather quickly large shifts, while EWMA and CUSUM charts are faster in detecting smaller shifts of the order 0.5σ. If the aim is to detect moderate to large jumps so called jump-preserving procedures are attractive, which are special cases of the unifying vertically weighted regression approach studied by Pawlak and Rafajłowicz (1999), Steland (2005), and Pawlak, Rafajłowicz, and Steland (2004, 2008). Nonparametric kernel control charts and the optimization for certain out-of-control models covering mixing processes have been studied in Steland (2004) and Steland (2005). Further, Wu and Spedding (2000) combined a classic Shewhart chart and a conforming run length chart yielding smaller ARLs for shifts larger than 0.8σ, but that method is inferior to the EWMA chart for smaller shifts.

The purpose of this paper is to propose a new binary chart, which is easy to apply, has enlarged sensitivity to very small shifts, and is robust with respect to deviations from normality. We provide a comprehensive study covering the methodology, asymptotic theory, practical issues of control chart design, and extensive Monte Carlo simulations.

Our study is motivated as follows: Although computing power has considerably increased, many practical applications still require detection procedures which are extremely fast to calculate. An example, which motivated our investigation, is the surveillance of copper production as outlined in Pawlak, Rafajłowicz, and Steland (2008). Here the problem is to detect defects and cracks resulting in lower quality. The copper is surveyed by a camera taking many high-resolution images per second, and each column of an image is analyzed in real time to detect defects. Only detectors which are fast enough to calculate can be employed. In such engineering image processing and image analysis applications one has to deal with the spatial inhomogeneity of the grey level of pixels. One can either assume that the inhomogeneity is compensated by a quite wiggly mean function which is disturbed by independent noise, or assume a smooth mean function overlayed by dependent noise. In the latter case fitting complex models to take account of dependencies is often not feasible in real-time applications. Then it is important to know how the chosen method behaves for dependent data. Let us also mention a further important area, namely the application of monitoring procedures to financial data. In financial statistics various empirical analyzes have revealed that asset returns are usually uncorrelated but the squares are serially correlated and are affected by conditional heteroscedasticity which produces the clusters of strongly dispersed returns seen in real data. Various models for returns assume or imply the martingale difference property.

Having in mind the above applications, we propose a simple method where one thresholds the observations to obtain binary data and applies a control chart based on the number of data points exceeding the threshold. In contrast to the classic Np-chart, the chart uses a finite *buffer* storing only the most recent observations. Our simulation results indicate that such a modified p-chart with a reduced number of observations reacts on average slower than several control charts studied recently in Han and Tsung (2004) for shifts larger than 0.25σ, but provides faster detection for very small shifts.

We provide an appropriate theoretical framework and prove a functional central limit theorem which shows that the classic Np chart's sensitivity with respect to very small shifts indeed can be improved by taking less observations into account. As argued above, the question arises, whether the result still holds true when the independence assumption underlying the classic p chart is dropped. The answer is positive: Our main result and its interpretation holds true for a large class of dependent processes, namely the class of triangular arrays of random variables forming a martingale difference array with respect to some filtration. Thus, the benefits of the modified p chart are also effective when monitoring dependent data.

The paper is organized as follows. In Section 2, we introduce the proposed control chart and its relationship to the classic Np-chart. An appropriate change-point model with local alternatives is introduced in Section 3 to study the problem from an asymptotic viewpoint. We establish a functional central limit theorem for the underlying stochastic process which induces the stopping time of interest. A proof of the main result is postponed to an appendix. Practical issues of control chart design are discussed in detail in Section 4. Finally, an extensive Monte Carlo study is presented in Section 5 providing a comparison with recently proposed control charts.

2 Statistical model and a modified p-chart

Our aim is to construct a control chart for detecting a shift of an unknown size m allowing for an unknown distribution F of the error terms. It is required that the in-control average run length (in-control ARL) of the chart can be tuned to sufficiently large values in order to reduce the number of false alarms. Simultaneously, the out-of-control ARL should be small, leading to quick detection of the jump after its occurrence. For a discussion of the design of control limits and their relationship to alarm rates and ARLs we refer to Margavio et al. (1995).

Even if the underlying distribution is normal, the Shewhart control chart is not powerful for detecting small changes, say m of the order of 0.1σ to 0.25σ, if σ denotes the standard deviation of the errors. The EWMA (exponentially weighted moving average) control chart is better suited to this purpose, but its performance is still not satisfactory in the range of very small shifts. For this reason a number of modifications of the Shewhart, EWMA, and

CUSUM charts have been proposed recently (see Han and Tsung (2004) and the bibliography cited therein). However, the design of a concrete control procedure with specific properties requires knowledge of the error distribution.

2.1 Change-point model

In this paper, we consider a classic change-point model, where the observations are of the form

$$Y_n = Y + m \cdot \mathbf{1}(n - q) + \varepsilon_n, \quad n = 1, 2, \dots \tag{1}$$

Y denotes the desired level of quality (target value) which is disturbed by random errors ε_n's. The deterioration of quality is modelled by jump (permanent shift in the quality characteristic) of height $m \neq 0$, which appears at time instant $q > 0$. q is called *change-point* and is assumed to be non-stochastic but unknown. $\mathbf{1}(t)$ denotes the indicator function on the set $[0, \infty)$, i.e.,

$$\mathbf{1}(t) = \begin{cases} 0 & if \quad t < 0 \\ 1 & if \quad t \geq 0 \end{cases}. \tag{2}$$

Thus, starting at the change-point q there is a jump of height m. In Section 3 we consider a change-point model allowing for jump sizes tending to 0 at a certain rate.

To simplify the exposition, we shall assume $Y = 0$ in what follows. For the same reason, let us tentatively assume that the error terms ε_n in (1) are independent and identically distributed random variables. That assumption will be relaxed in the next section. Whereas classic procedures are restricted to normally distributed noise, we allow for arbitrary distribution functions F which are symmetric about 0, i.e.,

$$F(x) = 1 - F(-x), \quad x \in \mathbb{R}. \tag{3}$$

Particularly, we allow for distributions having no finite expectations, e.g., the Cauchy distribution which has heavier tails than the normal distribution, or the Laplace (double exponential) law with lighter tails. Note that we do not require the error terms to possess a density f, but if they do, (3) implies $f(x) = f(-x)$.

2.2 The binary control chart revisited

The classic nonparametric Np-chart is distribution-free under quite general assumptions, and therefore is applicable when the error distribution is unknown. Although we confine our discussion to the case that the change from the in-control to the out-of-control scenario is given by a sharp jump, our approach can also be used for more general scenarios, because the construction of the control chart does not require knowledge of the underlying error distribution. As we shall see below, the chart proposed in this article provides noticeably

smaller out-of-control ARL than the classical and recently proposed control charts, but only for very small shifts, which are of the order 0.1-0.25 standard deviation – or its equivalent, based on the interquartile range, if the variance does not exists. A large number of theoretical investigations and computer simulations are witness of the fact that one can not expect existence of one "universal" chart with best performance in the whole range of shifts in the mean, if underlying distribution jump height are not specified. From this point of view, the binary chart occupies the region of small shifts.

Let us briefly review the definition and basic properties of the classic $N p$-chart. Obviously, if the process (1) is in-control and (3) holds, then – roughly – half of the observations should be positive and the rest are expected to be negative. In other words, having $N > 1$ observations

$$ Z_n \stackrel{def}{=} \text{sign}(Y_n) = \begin{cases} 0 & if \quad Y_n < 0 \\ 1 & if \quad Y_n \geq 0 \end{cases}, \quad n = 1, 2, \ldots, N \tag{4} $$

and introducing the counting random variable

$$ I_N \stackrel{def}{=} \text{card}\{Z_i = 1, \ i = 1, 2, \ldots, N\} = \sum_{i=1}^{N} Z_i \tag{5} $$

we have $\mathbb{E}(I_N) = N/2$, since I_N is a binomial random variable corresponding to N trials and success probability $p_0 = 1/2$. Here and in the sequel $\mathbb{E}$ denotes the expectation.

If a shift of size m occurred, then the distribution of subsequent Y_n's is no longer symmetric around zero and the probability of $Z_n = 1$ changes to

$$ p_1 = 1 - F(-m) \tag{6} $$

where p_1 can be larger or smaller than $1/2$, depending on whether m is positive or negative. Summarizing, one can detect a shift m by testing the hypothesis $H_0 : p_0 = 1/2$ against the alternatives that the success probability in one trial is different than $1/2$.

If the process is in-control, the dispersion of the binomial r.v. I_N equals $\sqrt{N p_0 (1 - p_0)}$. Then, I_N/N has expectation p_0 and dispersion $\sqrt{p_0 (1 - p_0)/N}$. Approximating the binomial distribution by the corresponding normal law we arrive at the well known $N p$-chart with upper control limit

$$ \text{UCL} = p_0 + k \sqrt{p_0 (1 - p_0)/N} \tag{7} $$

and the lower control limit (LCL)

$$ \text{LCL} = p_0 - k \sqrt{p_0 (1 - p_0)/N}, \tag{8} $$

where k is selected according to required averaged run length (ARL) in-control, the standard choice being $k = 3$. If I_N/N is outside the interval (LCL, UCL), then the out-of-control state

is claimed. Repeating the above reasoning, we can obtain the $N\,p_0$ version of this chart with the following control limits for I_N

$$N p_0 \pm k \sqrt{N\, p_0\,(1 - p_0)}, \tag{9}$$

where k is selected as above. For further discussions we refer to Montgomery (2001).

2.3 Modified p chart

The above chart is the starting point for our modifications. They are necessary, since the classical chart (Montgomery, 2001, pp. 284-294) is based on counting nonconforming items in samples of size N, which are either taken daily or at N consecutive days, if only one observation is available at each day. In the latter case, which is the setting we have in mind, the chart is applied only each Nth time instance. This can yield substantially larger delays in detection. Obviously, such sampling schemes are not appropriate for our purposes. Thus, we shall modify the chart in such a way that it counts a fixed number, $M > 1$ say, previous individual observations $Z_n = 1$ in a moving window. If the process is in-control, then we expect that about $M/2$ observations correspond to $Z_n = 1$.

More formally, we form a finite buffer of the length M, which contains only M past observations, excluding the latest one Z_n. M is called *buffer length*. When observation Z_n is available, it replaces Z_{n-1}, which is pushed to replace Z_{n-2} and so on. At each time instant n the present buffer contents is used to verify whether the process is in-control. To fix this idea, define the number of positive observations contained in the buffer in time n

$$J_n \;=\; \mathrm{card}\{Z_i = 1, i = (n-1), \dots, n - M\} = \sum_{i=n-M}^{n-1} Z_i. \tag{10}$$

Note that the difficulty with an initial content of the buffer appears. The proposed modified p-chart is built on the assumption that historical pre-run data are available which are known to form a random sample of the in-control process. Thus, in the sequel we assume that at time $n = 0$ the buffer contains past observations of the in-control process, which are numbered as $Z_{-1}, \dots, Z_{-M}$. Formally, we start the chart at $n = 0$, when the observation Z_0 arrives. Then, for $n = 1, 2, \dots$ it is verified whether the control statistic J_n lies between the control limits

$$\mathrm{UCL} \;=\; M\, p_0 \,+\, k \sqrt{M\, p_0\,(1 - p_0)}, \tag{11}$$

and

$$\mathrm{LCL} \;=\; M\, p_0 \,-\, k \sqrt{M\, p_0\,(1 - p_0)}. \tag{12}$$

Clearly, for $p_0 = 1/2$ these formulas simplify to $\mathrm{UCL} = M/2 + k\sqrt{M}/2$ and $\mathrm{LCL} = M/2 - k\sqrt{M}/2$. If J_n is smaller than LCLor larger than UCL, then out-of-control state is signaled. Note that the difference between UCLand LCLis constant for this chart.

6

The main difference between the proposed chart and the classical one can be summarized as follows. The classical Np chart is based on samples of size N from *non-overlapping* production intervals. In contrast, our chart counts events $Z_n = 1$ in the buffer on length M, which is moving forward with n, in such a way that new observation Z_n enters the buffer, while the oldest one is pushed out of it. In other words, the content of the buffer at time n and at time $n + 1$ highly overlap.

3 Asymptotic results

We will now present some asymptotic theory for the proposed procedure providing an explanation of the superiority of the modified p chart for small jumps. To simplify exposition, we slightly change the setting: We confine our study to a truncated version of the one-sided control chart which gives a signal if J_n exceeds UCL for some $1 \leq n \leq N$. However, our results can be extended to deal with the general case as outlined in Steland (2008). The small jump setting will be modelled by an appropriate asymptotic change-point model assuming a local alternative for the probabilities resp. jump heights.

To simplify our exposition, we introduce a maximum sample size N where monitoring stops in any case. Let us also rescale time by the transformation $t \mapsto \lfloor Nt \rfloor$, $t \in [0, 1]$, where $\lfloor x \rfloor$ denotes the largest integer smaller or equal to x, $x \in \mathbb{R}$. In the sequel, the current time point n will correspond to t, i.e., $n = \lfloor Nt \rfloor$.

Define the process

$$\mathcal{J}_N(t) = \frac{1}{\sqrt{N}} \sum_{i=\lfloor Nt \rfloor - M}^{\lfloor Nt \rfloor - 1} (Z_i - p_0), \qquad t \in [(M+1)/N, 1].$$

Note that $\mathcal{J}_N(n/N)$ is equal to the statistic J_n centered at its in-control expectation and scaled by $N^{-1/2}$. Now, the truncated version of the upper control chart of the last section, which gives a signal if J_n exceeds UCL, corresponds to the stopping time

$$S_N = \min\{M + 1 \leq n \leq N : J_n > Mp_0 + k\sqrt{Mp_0(1 - p_0)}\}.$$

We can represent S_N via the process $\mathcal{J}_N(t)$. Indeed, we have

$$S_N = N \inf\left\{ t \in [(M+1)/N, 1] : \mathcal{J}_N(t) > k\sqrt{\frac{M}{N}p_0(1 - p_0)} \right\}, \qquad N \geq 1. \tag{13}$$

For the asymptotic framework in this section, let us assume that the buffer length, M, is chosen as a $\mathbb{N}$-valued function of $n = \lfloor Nt \rfloor$, i.e., $M = M_{\lfloor Nt \rfloor}$, satisfying the growth condition

$$\frac{M_{\lfloor Nt \rfloor}}{N} \to M(t), \tag{14}$$

as the maximum sample size N tends to ∞. Here $M : [0,1] \to [0,1]$ is a non-decreasing function which is continuous on $(0,1]$ with $M(0) = 0$. We will call M *asymptotic buffer length (strategy)*. Condition (14) ensures that, asymptotically, the buffer length M is not too small compared to N.

To ensure that the buffer is not longer than the available time series, we impose the following condition.

Assumption (N): The buffer length strategy $M : [0,1] \to [0,1]$ satisfies the *natural condition*

$$M(t) \leq t \qquad \text{for all } t \in [0,1].$$

We shall show that under the following assumption the modified chart is superior to the classic one.

Assumption (M): The buffer length strategy satisfies the *modifier condition*, if

$$M(t) < t \qquad \text{for all } t \in (0,1], \tag{15}$$

Let us now consider some examples.

Example 3.1. *Put $M(0) = 0$ and $M_{\lfloor Nt \rfloor} = \lfloor \xi t N \rfloor$, $t \in (0,1]$, for some $\xi \in (0,1]$. Obviously, the natural condition (N) is satisfied, iff. $\xi < 1$. Particularly, the classic Np chart is given by $M_{\lfloor Nt \rfloor} = \lfloor Nt \rfloor$, $t \in [0,1]$, thus corresponding to $\xi = 1$ and $M(t) = t$, $t \in [0,1]$.*

The following example considers the case that the buffer lengths M_n are constant with respect to n.

Example 3.2. *Suppose $M_{\lfloor Nt \rfloor} = \lfloor \eta N \rfloor$ for some constant $\eta \in (0,1]$. For $t \in [0, \eta/N]$ the available data $Y_1, \ldots, Y_{\lfloor Nt \rfloor}$ do not fill the buffer. One may assume that pre-run data $Y_{-M+1}, \ldots, Y_0$ are available. However, to ensure a fair comparison with the classic Np chart, let us consider the choice*

$$M_{\lfloor Nt \rfloor} = \begin{cases} 0, & \lfloor Nt \rfloor < \lfloor N\eta \rfloor, \\ \lfloor \eta N \rfloor, & \lfloor Nt \rfloor \geq N\eta, \end{cases}$$

yielding $M(t) = \eta \mathbf{1}_{[\eta,1]}(t)$, $t \in [0,1]$. Alternatively, one may set

$$M_{\lfloor Nt \rfloor} = \min(\lfloor Nt \rfloor, \lfloor N\eta \rfloor)$$

yielding $M(t) = \min(t, \eta)$. Now the modified chart does not require historical data at the beginning. It starts as the classic chart and is modified as time proceeds to catch small late changes better.

Let us now consider an appropriate asymptotic change-point model for a small jump at location q. Assume that

$$\mu_{Ni} = \mathbb{E}(Z_i) = \begin{cases} p_0, & i < q = \lfloor N\vartheta \rfloor, \\ p_1, & i \geq q, \end{cases} \tag{16}$$

8

for some constant $\vartheta \in (0,1)$ which specifies the fraction of the maximum sample size N where the jump occurs. We model the out-of-control probability p_1 as a sequence of local alternatives given by

$$p_1 = p_{N1} = p_0 + \Delta/\sqrt{N},$$

such that $\Delta = \sqrt{N}(p_1 - p_0) > 0$.

Note that this model yields a triangular array of observations,

$$Z_{Ni}, \quad 1 \le i \le N, \quad N \ge 1,$$

where for each N the random variables $Z_{N1}, \dots, Z_{NN}$ are independent with $\mathbb{E}(Z_{Ni}) = p_0$ for $1 \le i < q$ and $\mathbb{E}(Z_{Ni}) = p_{N1}$ for $q \le i \le N$. Below we shall drop the independence assumption.

Remark 3.1. *For our purposes it is appropriate to formulate the change-point model in terms of the probabilities p_0 and p_1, but let us briefly discuss how it relates to a model for the jump height m. Assume the underlying probability density $f(x)$ is continuous and bounded in a neighborhood of 0. If we consider a local alternative model for the jump height where $m_N = \Delta_m/\sqrt{N}$ for a positive constant Δ_m, (6) and the mean value theorem give*

$$p_1 - p_0 = f(\xi_N)\Delta_m/\sqrt{N}$$

for points ξ_N between 0 and $\Delta_m/\sqrt{N}$. Thus, in this case

$$p_1 = p_0 + (f(0) + o(1))\Delta_m/\sqrt{N}.$$

In the sequel, $B(t)$, $t \in [0,1]$, denotes a standard Brownian motion with $B(0) = 0$, i.e., a centered Gaussian process with covariance function $\text{Cov}(B(s), B(t)) = \min(s,t)$, $s, t \in [0,1]$. The process $\mathcal{J}_N(t)$, $t \in [0,1]$, is an element of the Skorohod space $D[0,1]$ of all functions $f : [0,1] \to \mathbb{R}$ which are right-continuous with existing limits from the left. We denote distributional convergence (weak convergence) for a sequence $\{X, X_n\} \subset D[0,1]$ by $X_n \Rightarrow X$, as $n \to \infty$. For details we refer to Billingsley (1991) and Shorack (2000).

Our main result works under very general assumptions. Indeed, it just requires that the random variables $Z_{Ni} - \mu_{Ni}$ form a martingale difference array with $\mathbb{E}(Z_{Ni}^r | \mathcal{F}_{N,i-1}) = \mu_{Ni}$ for all i and $r = 1, 2$, for some filtration $\{\mathcal{F}_{Ni}\}$. In this case, the expectation in (16) is replaced by the conditional expectation $\mathbb{E}(Z_{Ni} | \mathcal{F}_{N,i-1})$. Recall that an array $\{X_{n,m} : 1 \le m \le n_k, n \ge 1\}$ of random variables defined on a common probability space $(\Omega, \mathcal{F}, \mathbb{P})$ is called *martingale difference array* with respect $\{\mathcal{F}_{n,m}\}$, if $\{\mathcal{F}_{n,m}\}$ forms a *filtration*, i.e.,

$$\mathcal{F}_{n,0} = \{\emptyset, \Omega\} \subset \mathcal{F}_{n,1} \subset \cdots \subset \mathcal{F}_{n,n_k} \subset \mathcal{F},$$

each $X_{n,m}$ is $\mathcal{F}_{n,m}$-measureable, and $\mathbb{E}(X_{n,m} | \mathcal{F}_{n,m-1}) = 0$ for all $1 \le m \le n_k$ and $n \ge 1$.

The martingale difference assumption is a natural approach to deal with time series. However, it is also suited and general enough to treat (locally) dependent image data, as demonstrated by the following example working with *sliced rectangular neighborhoods*.

Example 3.3. (A MODEL FOR LOCALLY DEPENDENT IMAGE DATA)
Suppose each column of an image consisting of I columns and J rows is analyzed from bottom to top. Assume the origin $(0,0)$ corresponds to the lower left corner and the pixels are denoted by $(i,j) \in \mathcal{I} \times \mathcal{J} = \{0, \dots I\} \times \{0, \dots, J\}$ for integers I, J. Let $\{\xi_{ij} : (i,j) \in \mathcal{I} \times \mathcal{J}\}$ be an array of i.i.d. random variables with common d.f. F satisfying $\mathbb{E}(\xi_{ij}) = 0$ and $\mathrm{Var}\,(\xi_{ij}^2) = 1$ for all $(i,j) \in \mathcal{I} \times \mathcal{J}$, representing the background noise of an image. For $h \geq 1$ define a sliced h-neighborhood for the pixel (i,j) by

$$\mathcal{N}_{ij} = \{(k,l) \in \mathcal{I} \times \mathcal{J} : (k = i \wedge l \leq j) \vee (1 \leq |i - k| \leq h \wedge l \leq j + h)\}$$

and denote by $\Xi_{ij} = \{\xi_{kl} : (k,l) \in \mathcal{N}_{ij}\}$ the corresponding set of ξ_{kl}'s. $\mathcal{N}_{ij}$ is a rectangle with width $2h+1$ and height $j+h$, sliced along the line from (i,j) to $(i,j+h)$. Then $\mathcal{N}_{i1} \subset \cdots \subset \mathcal{N}_{iJ}$, and consequently the family

$$\mathcal{F}_{i0} = \{\emptyset, \Omega\}, \quad \mathcal{F}_{ij} = \sigma(\Xi_{ij}) = \sigma(\xi_{kl} : (k,l) \in \mathcal{N}_{ij}),$$

defines a filtration. For what follows, notice that ξ_{ij} is not an element of the set $\Xi_{i,j-1}$. Let us now assume that the errors disturbing the true image are given by the model equations

$$\varepsilon_{ij} = h_{ij}\xi_{ij}, \qquad (i,j) \in \mathcal{I} \times \mathcal{J}, \qquad j = 2, \dots, J,$$

for $\mathcal{F}_{i,j-1}$-measureable random variables h_{ij} with existing second moments. Then $h_{ij} = H_{ij}(\Xi_{i,j-1})$ for functions H_{ij}. Obviously, ε_{ij} is $\mathcal{F}_{ij}$-measureable and, since ξ_{ij} is independent from the random variables of the set $\Xi_{i,j-1}$, we have $E(\xi_{ij}|\mathcal{F}_{i,j-1}) = E(\xi_{ij}) = 0$ yielding

$$\mathbb{E}(\varepsilon_{ij}|\mathcal{F}_{i,j-1}) = h_{ij}E(\xi_{ij}) = 0.$$

Thus, $\{\varepsilon_{ij} : (i,j) \in \mathcal{I} \times \mathcal{J}\}$ is a martingale difference array, and $\{\varepsilon_{ij} : j \in \mathcal{J}\}$ is a martingale difference sequence with respect to $\{\mathcal{F}_{ij} : j = 0, \dots, J\}$ for each $i \in \mathcal{I}$. Since

$$\mathrm{Var}\,(\varepsilon_{ij}|\mathcal{F}_{i,j-1}) = h_{ij}^2,$$

h_{ij}^2 is the conditional variance given the neighboring pixels. Particularly, h_{ij}^2 may depend on the noise levels of these neighboring pixels. Recall that when the kth column is analyzed, Z_{Ni} is given by $Z_{Ni} = \mathbf{1}(\varepsilon_{ki} \leq 0)$ for $i = 1, \dots, N = J$. We have

$$\mathbb{E}(Z_{Ni}|\mathcal{F}_{k,i-1}) = \mathbb{P}(h_{ik}\xi_{ik} \leq 0|\mathcal{F}_{k,i-1}) = F(0/h_{ik}) = p_0 = 1/2.$$

and $\mathrm{Var}\,(Z_{Ni}|\mathcal{F}_{k,i-1}) = p_0(1-p_0)$. Consequently, the random variables $Z_{Ni} - p_0$, $i = 1, \dots, N$, also form a martingale difference array with respect to the filtration $\{\mathcal{F}_{ki} : i = 1, \dots, N\}$ with common conditional variance $p_0(1 - p_0)$.

We are now in a position to formulate our main result concerning the weak convergence of the process $\mathcal{J}_N(t)$ and the corresponding central limit theorem for the modified chart.

Theorem 3.1. *Suppose (N) and that the random variables $\xi^*_{Ni} = (Z_{Ni} - \mu_{Ni}))/\sqrt{\mu_{Ni}(1 - \mu_{Ni})}$ form a martingale difference array with respect to some filtration $\mathcal{F}_{Ni}$, such that*

$$\mathbb{E}(\xi^*_{Ni}|\mathcal{F}_{N,i-1}) = 0 \qquad and \qquad \mathrm{Var}\,(\xi^*_{Ni}|\mathcal{F}_{N,i-1}) = 1,$$

for all $1 \le i \le N$, $N \ge 1$. Then the following conclusions hold true.

(i) *If there is no change-point, the process $\mathcal{J}_N$ converges weakly,*

$$\mathcal{J}_N(t) \Rightarrow \eta_0[B(t) - B(t - M(t))],$$

as $N \to \infty$, where

$$\eta_0^2 = \lim_{N \to \infty} Var\left(N^{-1/2}\sum_{i=1}^{N}(Z_{Ni} - \mathbb{E}(Z_i))\right) = p_0(1 - p_0).$$

The normed stopping time converges in distribution,

$$S_N/N \xrightarrow{d} \tau_M$$

where

$$\tau_M = \inf\{t \in [0,1] : B(t) - B(t - M(t)) > k\sqrt{M(t)}\}$$

(ii) *Under the local change-point model (16), the process $\mathcal{J}_N$ converges weakly,*

$$\mathcal{J}_N(t) \Rightarrow \mathcal{J}_M^{(1)}(t) = \begin{cases} \eta_0[B(t) - B(t - M(t))], & t < \vartheta, \\ \eta_0[B(t) - B(t - M(t))] + (t - \vartheta)\Delta, & \vartheta \le t < \vartheta + M(t), \\ \eta_0[B(t) - B(t - M(t))] + M(t)\Delta, & \vartheta + M(t) \le t, \end{cases}$$

as $N \to \infty$. The normed stopping time converges in distribution,

$$S_N/N \xrightarrow{d} \tau_M^{(1)} = \inf\{s \in [0,1] : \mathcal{J}_M^{(1)}(s) > k\sqrt{M(s)}\eta_0\}.$$

Remark 3.2. *Notice that the standard i.i.d. setting, where it is assumed that $Z_{N1}, \ldots, Z_{NN}$ are independent and identically distributed Bernoulli variables with success probability p_0, is covered as a special case.*

The above theorem says that, asymptotically, the control chart behaves as the stopping time τ_M which is driven by the stochastic process

$$\mathcal{V}(t) = B(t) - B(t - M(t)).$$

Notice that the one-dimensional marginals of $\mathcal{V}(t)$ are distributed as $B(M(t))$. Further, for $s \leq t$ we have

$$E\mathcal{V}(s)\mathcal{V}(t) = \begin{cases} 0, & s - M(s) \leq s \leq t - M(t) \leq t, \\ s - t + M(t), & s - M(s) \leq t - M(t) \leq s \leq t, \\ M(s), & t - M(t) \leq s - M(s) \leq s \leq t. \end{cases}$$

For small values of $|s-t|$, i.e., locally, the process $V(t)$ behaves similar as the process $B(M(t))$, if $M(t)$ is a smooth function.

The above theoretic results explain the benefits from using the modified binary chart: Assume (M) and suppose a signal is given at time $t \in [\vartheta, \vartheta + M(t))$ where $\eta \leq \vartheta$ (cf. Example 3.2.) In this case

$$\frac{\mathcal{V}(t)}{\sqrt{M(t)}} + \frac{(t - \vartheta)\Delta}{\eta_0 \sqrt{M(t)}} > k.$$

Right before the threshold k is hit, the behavior of the random part of the left hand side can be approximated by the process $B(M(t))/\sqrt{M(t)}$, which has expectation 0, variance 1 for any function $M(t)$, and covariance function

$$(s, t) \mapsto \frac{\min(M(s), M(t))}{\sqrt{M(s)M(t)}}.$$

For small values of $|s-t|$ and smooth $M(t)$ this is approximately a Brownian motion. Consider the drift term $(t - \vartheta)\Delta/(\eta_0 \sqrt{M(t)})$, which mainly yields the detection power. The modifier condition (M) ensures that the drift term is strictly larger than the drift term for the case $M(t) = t$ corresponding to the classic Np chart. This explains the superior performance of the modified chart for small jumps.

If the change was not detected until time $\vartheta + M(t)$, a signal is given if

$$\frac{\mathcal{V}(t)}{\sqrt{M(t)}} + \frac{\sqrt{M(t)}\Delta}{\eta_0} > k.$$

For the random part the same arguments as given above apply. But now under condition (M) the drift term is strictly smaller than the drift term for the case $M(t) = t$. We may summarize that the limit theorem indicates that the modified p chart is preferable to detect very small jumps right after the change-point.

Also notice that Theorem 3.1 yields well defined limit distributions for small jumps of the order $N^{-1/2}$. Clearly, for jumps of higher order, the drift diverges and dominates the random part, such that the beneficial effect of the function $M(t)$ is not visible.

4   Practical issues of control chart design

Unlike the classic Np-chart, the modified chart has two tunable parameters, namely, M and k, which should be carefully selected in order to ensure small out-of-control ARLs (average

run length to detection) under the constraint that the in-control ARL (average run length to false alarm) is not smaller than a given level.

We will now summarize our experience on tuning this chart by simulations, which are justified to some extent by the theoretical results presented in the previous section. The major issue is how to select the control limit.

(i) In practice, the 3σ rule is often advocated, i.e., $k = 3$. However, this is not advisable here, since it leads to excessively long in-control ARLs. For our control chart, the in-control ARL also depends on the buffer length M. Selecting $k = 2.34$ and $M = 9$ we get first reasonable in-control ARL about 500.

(ii) For a given buffer length the same in-control ARL is attained for k from a certain relatively long interval. This is due to the fact that J_n is always an integer.

(iii) Analysis of Figure 1, where log of in-control ARL is plotted as a function of k for different buffer lengths, reveals that it is advisable to select k at the left end of that interval. That choice ensures the specified in-control ARL and minimizes the distance $\mathrm{UCL} - \mathrm{LCL}$.

In view of these remarks we suggest the following practical approach to select the parameters M and k of the chart.

1. Select a desired in-control ARL, e.g., equal to 370.

2. Select the buffer length $M > 1$. A discussion on selecting M is presented below.

3. For a practical application one may simulate the in-control ARL for k varying from 1 to 3. It is not difficult to find a reasonable k in this way, but determining exactly the smallest k, which guarantees the specified in-control ARL is a computationally demanding task.

For the reader's convenience Table 1 summarizes some pairs (M, k) with minimal k (accuracy 0.01) ensuring an in-control ARL of approximately 435. Notice that in general the fact that J_n is integer-valued prevents the construction of a control chart with in-control ARL being equal to the target in-control ARL.

One may also select M to minimize the out-of-control ARL for a given jump height m. Figure 2 indicates that for jump heights $m = 0.25$, $m = 0.5$, and $m = 0.75$ there exist optimal buffer lengths M. The choices $M = 71$, $M = 28$, $M = 23$ are optimal for $m = 0.25$, $m = 0.5$, and $m = 0.75$, respectively, taking into account that the selection was made among a rather limited number of buffer lengths. Clearly, an exhaustive search may yield slightly better results. Note, however, that for $m = 1$ the plot is increasing and one might expect that
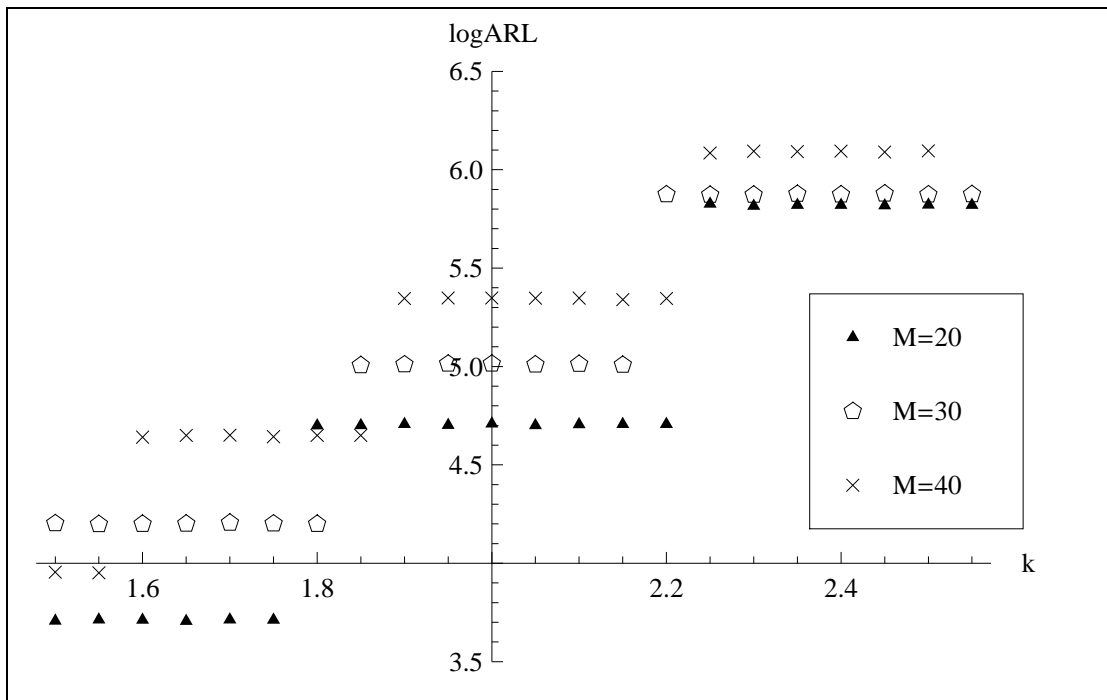
Figure 1: Dependence of the logarithm of the in-control ARL on the threshold k for different buffer sizes M. The results were obtained for Gaussian $N(0,1)$ errors by averaging 10^4 simulation runs.
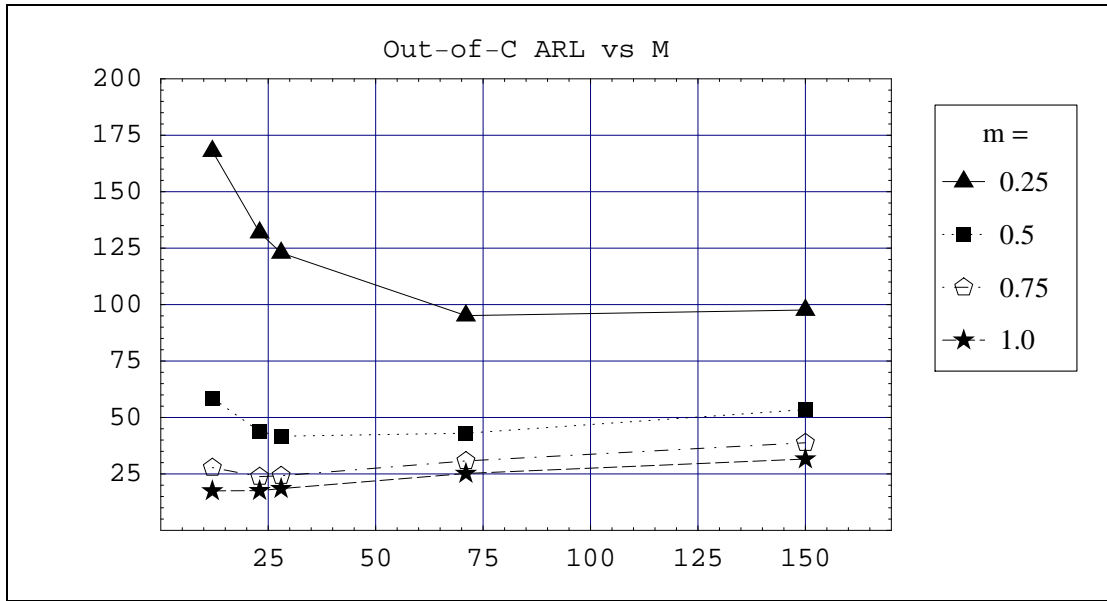
Figure 2: Dependence of the out-of-control ARL as a function of the buffer size M for different jump heights m and normal errors.

$M =$	12	23	28	71	90	150	212	441
$k =$	2.31	2.30	2.27	2.02	2.0	1.8	1.65	1.39
$ARL_0 =$	395	415	423	411	450	452	440	456

Table 1: Pairs of parameters (M, k) of the proposed chart ensuring an in-control ARL or the order 435.

the best choice is for $M < 12$, but in this region one can not attain in-control ARL of order 435.

5 Simulation studies

We performed extensive simulations aiming at the following issues. Firstly, we were interested in identifying pairs of the buffer length M and the threshold k ensuring a specified in-control ARL (at least approximately). Secondly, we investigated the out-of-control ARL for various jump heights, when the underlying observations are normally distributed. Third, we compared the binary chart with other charts for the case of normally distributed error terms, focusing on the out-of-control ARL as a performance measure. Finally, we studied the behavior of the out-of-control ARL for the binary chart when the errors are non-normal.

The simulation results are given in the tables below. All the results were obtained by averaging 30000 simulation runs. Simulated jump occured at time zero and the buffer was fed up by in-control pre-run observations. The results of simulation studies can be summarized as follows.

(i) For Gaussian errors and an out-of-control ARL fixed at 435, our chart with buffer length $M = 150$ (see Table 3) provides shorter out-of-control ARL's than CUSUM, Optimal EWMA, Shewhart-EWMA, GEWMA and GLR (see Han and Tsung (2004) for definitions), provided the jump is small. To be precise, the out-of-control ARL of our chart is about 243 for a jump $m = 0.1\,\sigma$, and about 97 for $m = 0.25\,\sigma$, while for the above mentioned charts we have ARL's between 295 and 324 and between 105 and 110, respectively. Simultaneously, the dispersion of the RL time of our chart is considerably smaller and equals 172 for $m = 0.1\,\sigma$ and about 59 for $m = 0.25\,\sigma$, while for the charts discussed in Han and Tsung (2004) we have RL time dispersions of the orders 267-324 and 79-102, respectively.

(ii) Qualitatively the same pattern can be observed when the out-of-control ARL is fixed at 840 and errors are Gaussian (see Table 4 and Han and Tsung (2004)).

(iii) When the jump is larger than $0.5\,\sigma$, the proposed chart is much slower than the above mentioned charts, but this shortcoming can easily be handled by applying several charts simultaneously and claiming an alarm when one of them gives a signal.

(iv) The proposed chart retains its advantages in the range of small jumps when the errors are double exponentially distributed and even behaves quite well for difficult distributions as the Cauchy one (see Table 5).

Acknowledgments

A   Proof of the main result

Under the change-point model of Section 3 we are given an array $\{Z_{Ni} : 1 \leq i \leq N, N \geq 1\}$ of Bernoulli variables with conditional expectations $\mathbb{E}(Z_{Ni}|\mathcal{F}_{N,i-1}) = p_0$ if $1 \leq i < \lfloor N\vartheta \rfloor$, and $\mathbb{E}(Z_{Ni}|\mathcal{F}_{N,i-1}) = p_{N1} = p_0 + \Delta/\sqrt{N}$ if $\lfloor N\vartheta \rfloor \leq i \leq N$, $N \geq 1$.

Theorem A.1. *(Durrett 2005, Theorem 7.3). Suppose $\{X_{n,m}\}$ is a martingale difference array with respect to $\{\mathcal{F}_{n,m}\}$. Define*

$$S_{n,k} = \sum_{i=1}^{k} X_{n,i}, \qquad V_{n,k} = \sum_{1 \leq i \leq k} \mathbb{E}(X_{n,i}^2 | \mathcal{F}_{n,i-1}), \qquad 0 \leq k \leq n.$$

If

    (i) $V_{n,\lfloor nt \rfloor} \to t$ in probability for all $t \in [0,1]$ and

    (ii) for all $\varepsilon > 0$, $\sum_{m \leq n} \mathbb{E}(X_{n,m}^2 \mathbf{1}_{\{|X_{n,m}| > \varepsilon\}} | \mathcal{F}_{n,m-1}) \to 0$ in probability,

then $S_{n,\lfloor nt \rfloor} \Rightarrow B(t)$, where B denotes a standard Brownian motion.

Proof. (of Theorem 3.2) We first consider the case when there is no change. Let us introduce the partial sum process,

$$Z_N(t) = \sum_{i=1}^{\lfloor Nt \rfloor} \xi_{Ni}, \qquad t \in [0,1],$$

where $\xi_{Ni} = (Z_{Ni} - p_0)/\sqrt{Np_0(1-p_0)}$, $1 \leq i \leq N$. Let us first verify that the array $\{\xi_{Ni} : 1 \leq i \leq N, N \geq 1\}$ satisfies the assumptions of Theorem A.1. Clearly, $E(\xi_{Ni} | \mathcal{F}_{N,i-1}) = 0$ and

$$E(\xi_{Ni}^2 | \mathcal{F}_{N,i-1}) = \text{Var}\left(\xi_{Ni} | \mathcal{F}_{N,i-1}\right) = N^{-1},$$

for all $1 \leq i \leq N$, yielding

$$V_{N,\lfloor Nt \rfloor} = \sum_{i=1}^{\lfloor Nt \rfloor} E(\xi_{Ni}^2 | \mathcal{F}_{N,i-1}) = \frac{\lfloor Nt \rfloor}{N} \to t,$$

as $N \to \infty$. The conditional Lindeberg condition is shown as follows. Since $E((Z_{Ni} - p_0)^2 | \mathcal{F}_{N,i-1}) \leq 1$, $1 \leq i \leq N$, we obtain for any $\varepsilon > 0$

$$L_N(\varepsilon) = \sum_{i=1}^{N} E(\xi_{Ni}^2 \mathbf{1}(|\xi_{Ni}| > \varepsilon) | \mathcal{F}_{N,i-1})$$

$$\frac{1}{N} \sum_{i=1}^{N} E\left(\frac{(Z_{Ni} - p_0)^2}{p_0(1-p_0)} \mathbf{1}\left(\frac{|Z_{Ni} - p_0|}{\sqrt{p_0(1-p_0)}} > \varepsilon\sqrt{N} \right) \bigg| \mathcal{F}_{N,i-1} \right)$$

$$\leq \frac{1}{Np_0(1-p_0)} \sum_{i=1}^{N} P\left(\frac{|Z_{Ni} - p_0|}{\sqrt{p_0(1-p_0)}} > \varepsilon\sqrt{N} \bigg| \mathcal{F}_{N,i-1} \right).$$

The conditional Markov inequality yields for $1 \leq i \leq N$

$$P\left(\frac{|Z_{Ni} - p_0|}{\sqrt{p_0(1-p_0)}} > \varepsilon\sqrt{N} \bigg| \mathcal{F}_{N,i-1} \right) \leq \frac{1}{\varepsilon^2 N},$$

which implies
$$\lim_{N\to\infty} L_N(\varepsilon) = 0.$$

Hence, by Theorem A.1
$$Z_N \Rightarrow B, \qquad N \to \infty.$$

Now, as will be shown below for a more involved setting,
$$J_N(t) = \sqrt{p_0(1-p_0)} \left[Z_N(t - \frac{1}{N}) - Z_N(t - \frac{M_{\lfloor Nt \rfloor}}{N} - \frac{1}{N}) \right]$$
$$\Rightarrow \eta_0[B(t) - B(t - M(t))],$$

as $N \to \infty$. Having in mind the rule (13), we conclude
$$\mathcal{J}_N(t) - k\sqrt{M_{\lfloor Nt \rfloor} N^{-1} p_0(1-p_0)} \Rightarrow \eta_0[B(t) - B(t - M(t))] - k\sqrt{M(t)}\eta_0, \qquad N \to \infty,$$

which yields
$$S_N/N \xrightarrow{d} \inf\{s \in (0,1] : B(t) - B(t - M(t)) > k\sqrt{M(s)}\},$$

as $N \to \infty$.

To establish (ii), we consider three cases.

Case 1: $\lfloor Nt \rfloor \le \lfloor N\vartheta \rfloor$ is handled as above.

Case 2: $\lfloor N\vartheta \rfloor < \lfloor Nt \rfloor < \lfloor N\vartheta \rfloor + M_{\lfloor Nt \rfloor}$. Denote the set of corresponding values of t by $\mathcal{T}_2$. $\mathcal{J}_N(t)$ equals
$$\frac{1}{\sqrt{N}} \sum_{i=\lfloor Nt \rfloor - M_{\lfloor Nt \rfloor}}^{\lfloor N\vartheta \rfloor - 1} (Z_i - p_0) + \frac{1}{\sqrt{N}} \sum_{i=\lfloor N\vartheta \rfloor}^{\lfloor Nt \rfloor - 1} (Z_{Ni} - p_{N1}) + \frac{1}{\sqrt{N}} \sum_{i=\lfloor N\vartheta \rfloor}^{\lfloor Nt \rfloor - 1} (p_{N1} - p_0). \qquad (17)$$

Since $p_1 - p_0 = \Delta/\sqrt{N}$, the third term converges (pointwise) to the continuous function $\Delta(t - \vartheta)$, which implies that the convergence is also uniform in $t \in [\vartheta, \vartheta + M(t)]$. To handle the random terms put
$$\widetilde{\xi}_{Ni} = \begin{cases} (Z_i - p_0)/\sqrt{p_0(1-p_0)N}, & 0 \le i \le \lfloor N\vartheta \rfloor - 1, \\[2mm] (Z_{Ni} - p_{N1})/\sqrt{p_{N1}(1-p_{N1})N}, & \lfloor N\vartheta \rfloor \le i \le N. \end{cases}$$

Again, the conditions of the functional martingale central limit theorem are satisfied, such that $\widetilde{Z}_N(t) = \sum_{i=1}^{\lfloor Nt \rfloor} \widetilde{\xi}_{Ni} \Rightarrow B(t)$. The first and second term in (17) are now given by
$$\sqrt{p_0(1-p_0)} \left[\widetilde{Z}_N(\vartheta - \frac{1}{N}) - \widetilde{Z}_N(t - \frac{M_{\lfloor Nt \rfloor}}{N} - \frac{1}{N}) \right]$$
$$+ \sqrt{p_{N1}(1-p_{N1})} \left[\widetilde{Z}_N(t - \frac{1}{N}) - \widetilde{Z}_N(\vartheta - \frac{1}{N}) \right],$$

18

which equals $\varphi_N(\widetilde{Z}_N)(t)$, if we define the sequence of functionals $\varphi_N : (D[0,1], d) \to (D[0,1], d)$, $N \geq 1$, by

$$\varphi_N(z)(t) = \sqrt{p_0(1-p_0)}\left[z(\vartheta - 1/N) - z(t - \frac{M_{\lfloor Nt \rfloor}}{N} - \frac{1}{N})\right]$$
$$+ \sqrt{p_{N1}(1-p_{N1})}\left[z(t - \frac{1}{N}) - z(\vartheta - \frac{1}{N})\right].$$

Also define

$$\varphi(z) = \sqrt{p_0(1-p_0)}[z(t) - z(t - M(t))], \qquad z \in C[0,1].$$

By linearity, φ_N is uniformly Lipschitz continuous, i.e.,

$$\sup_{N \geq 1} \|\varphi_N(z_1) - \varphi_N(z_2)\|_\infty \leq L\|z_1 - z_2\|_\infty,$$

for all $z_1, z_2 \in D[0,1]$, where $L = 2\sup_{N \geq 1}\sqrt{p_{N1}(1-p_{N1})} < \infty$. Further, since any $z \in C[0,1]$ is uniformly continuous,

$$\|\varphi_N(z) - \varphi(z)\|_\infty \to 0, \qquad N \to \infty.$$

Let $\{z, z_N\} \subset D[0,1]$ be a sequence with $z_N \to z \in C[0,1]$ in the Skorohod metric, which implies $\|z_N - z\|_\infty \to 0$. Apply the triangle inequality to obtain

$$\|\varphi_N(z_N) - \varphi(z)\|_\infty \leq \|\varphi_N(z_N) - \varphi_N(z)\|_\infty + \|\varphi_N(z) - \varphi(z)\|_\infty.$$

The first term is bounded by $L\|z_N - z\|_\infty \to 0$, $N \to \infty$, and the second one tends to 0 by the uniform Lipschitz continuity. For $z \in C[0,1]$ we have $\varphi(z)(t) = \sqrt{p_0(1-p_0)}[z(t) - z(t - M(t))]$. Due to the Shorohod/Dudley/Wichura representation theorem, $\widetilde{Z}_N \Rightarrow B$, $N \to \infty$, implies that there exists a probability space and equivalent version of $\widetilde{Z}_N$ and B defined on that new space, which we again denote by $\widetilde{Z}_N$ and B, such that $\|\widetilde{Z}_N - B\|_\infty \to 0$, $N \to \infty$, a.s. The above arguments ensure that

$$\varphi_N(\widetilde{Z}_N)(t) \Rightarrow \varphi(B)(t) = \eta_0[B(t) - B(t - M(t))],$$

as $N \to \infty$.

Case 3: $\lfloor N\vartheta \rfloor + M_{\lfloor Nt \rfloor} \leq t$ is obvious.

Putting things together yields the result for $\mathcal{J}_N(t)$. Since the process $\mathcal{J}_M^{(1)}$ is a.s. continuous, we may further conclude that

$$S_N/N \xrightarrow{d} \tau_M^{(1)} = \inf\{t \in [0,1] : \mathcal{J}_M^{(1)}(t) > k\sqrt{M(t)}\eta_0\},$$

as $N \to \infty$. $\qquad\qquad\qquad\qquad\qquad\qquad\qquad\qquad\qquad\qquad\qquad\qquad\qquad\square$

References

Antoch J. and Jarušková M. (2002). On-line statistical process control, in: *Multivariate Total Quality Control, Foundations and Recent Advances*, ed. Lauro C., Antoch J., and Vinzi, V.E., Physica, Heidelberg.

Antoch J., Hušková M., and Jarušková M. (2002). Off-line statistical process control, in: *Multivariate Total Quality Control, Foundations and Recent Advances*, ed. Lauro C., Antoch J., and Vinzi, V.E., Physica, Heidelberg.

Billingsley, P. *Weak Convergence of Probability Measures*, 2nd ed., New York: Wiley, 1991.

Brodsky, B.E., and Darkhovsky, B.S. (2000). *Non-Parametric Statistical Diagnosis: Problems and Methods*. Dordrecht: Kluwer Academic Publishers.

Chakraborti S., van der Laan P., and Bakir S.T. (2001). Nonparametric control charts: An overview and some results, *J. Qual. Tech.*, vol. 33, 304-315.

Durrett, R. *Probability: Theory and Examples*, 3rd ed., Belmont: Brooks/Cole Thomson - Learning.

Han D., Tsung F. (2004). A generalized EWMA control chart and its comparison with the optimal EWMA, CUSUM and GLR schemes. *Ann. of Stat.*, 32, 316–340.

Margavio T.M., Conerly M.D., Woodall W.H., and Drake L.G. (1995). Alarm rates for quality control charts, *Statist. Probab. Lett.*, vol. 24, 219-224.

Montgomery D. C. (2001). *Introduction to Statistical Quality Control*. 4th Edition, New York: Wiley.

Munford A.G. (1980). A control chart based on cumulative scores, *Appl. Stat.*, vol. 29, 252-258.

Pawlak, M. and Rafajłowicz, E. (1999). Vertically weighted regression - a tool for nonlinear data analysis and constructing control charts. *J. German Statistical Association*, vol. 84, 367-388.

Pawlak, M., Rafajłowicz, E., and Steland A. (2004). On detecting jumps in time series - Nonparametric setting. *J. Nonparametr. Stat.*, vol. 16, 329-347.

———— (2008). Nonlinear image processing and filtering: A unified approach based on vertically weighted regression. *Intern. J. of Appl. Math. Comput. Sci.*, vol. 18, 1, 49-61.

Shorack, G.R. (2000). *Probability for Statisticians*, New York: Springer.

STELAND, A. (2004). Sequential control of time series by functionals of kernel-weighted empirical processes under local alternatives. *Metrika*, 60, 229-249.

———— (2005). Optimal sequential kernel smoothers under local nonparametric alternatives for dependent processes. *J. Stat. Planning and Inference*, 132, 131-147.

———— (2005). On the distribution of the clipping median under a mixture model. *Statist. Probab. Lett.*, 70 (1), 1-13.

———— (2008). Sequentially updated residuals and detection of stationary errors in polynomial regression models. *Sequential Anal.*, forthcoming.

WOODALL W.H. (1997). Control charts based on attribute data: Bibliography and review. *J. Qual. Tech.*, vol. 29, pp 172-183.

Wu Z. and Spedding T.A. A synthetic control chart for detecting small shifts in the process mean, *J. Qual. Tech.*, vol. 32, pp 32-38.

M= 12, k =2.31			M= 23, k =2.3			M= 28, k =2.27		
Jump	ARL	RL Disp,	Jump	ARL	RL Disp,	Jump	ARL	RL Disp,
0	395.27	171.09	0	415.66	181.42	0	423.12	185.75
0.1	328.33	144.18	0.1	305.80	133.14	0.1	303.43	133.17
0.25	168.09	72.47	0.25	131.89	56.00	0.25	122.90	51.72
0.5	58.65	24.52	0.5	43.78	17.08	0.5	41.66	15.73
0.75	27.84	10.91	0.75	23.76	8.35	0.75	24.18	8.27
1	17.51	6.35	1	17.60	5.76	1	18.53	6.00
1.25	12.98	4.41	1.25	14.99	4.76	1.25	16.10	5.12
1.5	10.96	3.54	1.5	13.66	4.31	1.5	14.76	4.68
1.75	10.00	3.14	1.75	12.88	4.05	1.75	13.99	4.42
2	9.46	2.94	2	12.45	3.91	2	13.54	4.28
2.25	9.19	2.84	2.25	12.26	3.84	2.25	13.25	4.18
2.5	9.09	2.80	2.5	12.12	3.80	2.5	13.14	4.14
2.75	9.05	2.79	2.75	12.04	3.77	2.75	12.96	4.09
3	9.01	2.77	3	11.96	3.75	3	13.09	4.12

Table 2: Binary chart applied to observations with Gaussian errors. Chart tuned to in-control ARL about 435. Short buffer length.

$M=$ 71, $k=$2.02			$M=$ 150, $k=$1.8			$M=$ 212, $k=$1.65		
Jump	ARL	RL Disp,	Jump	ARL	RL Disp,	Jump	ARL	RL Disp,
0	411.23	301.39	0	452.05	337.19	0	440.32	334.70
0.1	254.91	182.71	0.1	243.54	172.58	0.1	234.27	166.92
0.25	95.12	60.68	0.25	97.58	58.68	0.25	101.26	60.62
0.5	43.03	23.33	0.5	53.50	29.52	0.5	56.87	32.41
0.75	30.75	16.08	0.75	38.80	21.12	0.75	41.30	23.18
1	25.23	13.06	1	31.60	17.07	1	33.77	18.76
1.25	22.11	11.39	1.25	27.71	14.87	1.25	29.38	16.24
1.5	20.28	10.41	1.5	25.20	13.50	1.5	26.92	14.81
1.75	19.22	9.83	1.75	23.82	12.74	1.75	25.38	13.93
2	18.61	9.50	2	23.10	12.30	2	24.57	13.48
2.25	18.13	9.25	2.25	22.64	12.05	2.25	24.17	13.19
2.5	17.91	9.14	2.5	22.31	11.86	2.5	23.76	13.00
2.75	17.83	9.08	2.75	22.17	11.80	2.75	23.70	12.95
3	17.69	9.03	3	22.15	11.77	3	23.70	12.94

Table 3: Binary chart applied to observations with Gaussian errors. Chart tuned to in-control ARL about 435. Moderate and long buffer length.

M= 111, k =2.19			M= 131, k =1,84			M= 453, k =1.35		
Jump	ARL	RL Disp,	Jump	ARL	RL Disp,	Jump	ARL	RL Disp,
0	836.64	370.04	0	841.83	370.73	0	840.02	650.13
0.1	398.04	170.64	0.1	399.22	171.86	0.1	337.79	226.64
0.25	122.34	46.80	0.25	124.06	46.98	0.25	149.54	87.46
0.5	57.56	19.21	0.5	57.63	19.18	0.5	82.94	47.32
0.75	41.71	13.77	0.75	42.10	13.83	0.75	59.05	33.34
1	34.13	11.17	1	34.18	11.20	1	48.22	27.03
1.25	29.78	9.72	1.25	29.60	9.66	1.25	42.12	23.43
1.5	27.12	8.84	1.5	27.18	8.84	1.5	38.14	21.23
1.75	25.66	8.35	1.75	25.61	8.32	1.75	36.05	20.03
2	24.76	8.04	2	24.66	8.02	2	34.93	19.38
2.25	24.24	7.88	2.25	24.21	7.87	2.25	34.33	18.98
2.5	24.00	7.78	2.5	23.96	7.77	2.5	33.79	18.71
2.75	23.97	7.78	2.75	23.78	7.74	2.75	33.36	18.48
3	23.79	7.73	3	23.69	7.70	3	33.55	18.57

Table 4: Binary chart applied to observations with Gaussian errors. Chart tuned to in-control ARL about 840. Moderate and long buffer length.

Laplace (DblExp)			Cauchy		
$M = 40,\ k = 2.22$			$M = 28,\ k = 2.28$		
Jump	ARL	RL Disp,	Jump	ARL	RL Disp,
0	437.69	315.91	0	420.79	300.12
0.1	191.35	133.31	0.1	334.82	240.04
0.25	59.51	37.02	0.25	167.28	116.28
0.5	28.51	15.02	0.5	64.17	41.76
0.75	22.04	11.13	0.75	37.52	22.47
1	19.33	9.69	1	27.27	15.21
1.25	17.70	8.84	1.25	22.70	12.03
1.5	16.85	8.37	1.5	20.51	10.58
1.75	16.15	8.02	1.75	18.86	9.55
2	15.78	7.83	2	17.93	9.00
2.25	15.55	7.69	2.25	17.23	8.58
2.5	15.34	7.59	2.5	16.67	8.28
2.75	15.19	7.52	2.75	16.29	8.07
3	15.07	7.46	3	15.98	7.90

Table 5: Comparison of ARLs of the binary chart with in-control ARL 435 when applied to non-Gaussian distributions. 30, 000 independent simulation trials.